



# Finger Print History, Registration, Enhancement, and Minutias Detection

**Daniel Novák**

**5.10. 2023, Prague**

**Acknowledgments: Xavier Palathingal, Andrzej Drygajlo,  
Handbook of Fingerprint Recognition**

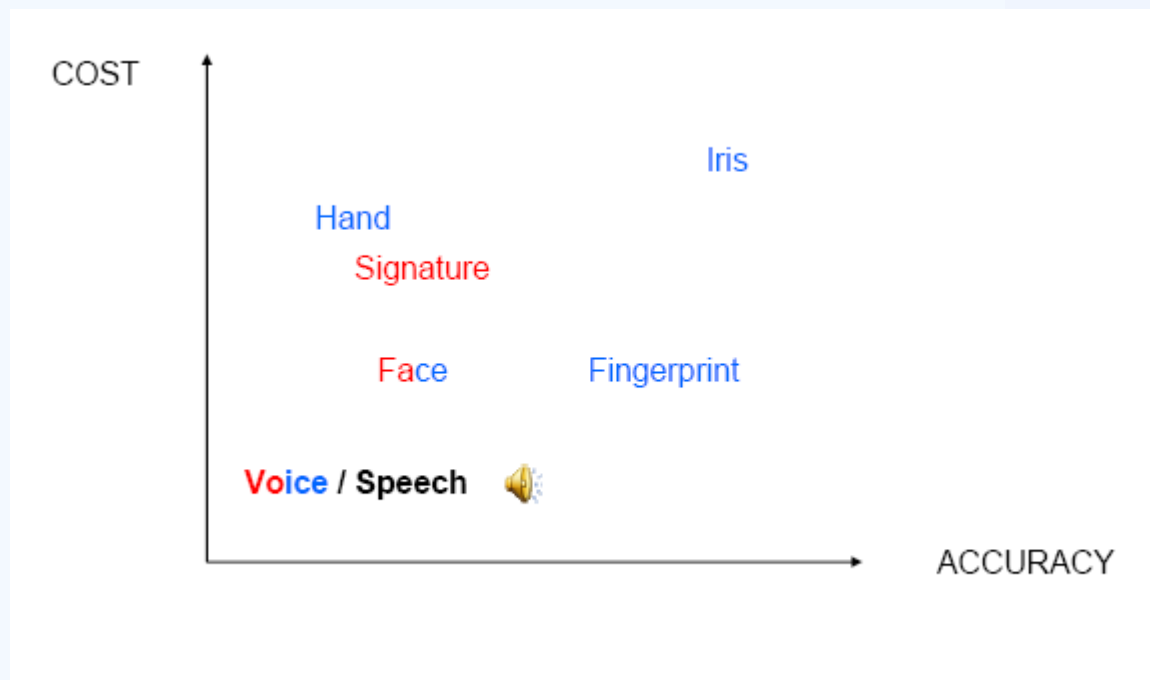


laboratory  
**Gerstner**



# Outline

- Introduction to Fingerprint
- History
- Registration
- Enhancement
- Minutiae detection



Capture

Extraction

Comparison

Verify individual?



Scan left index finger



Thin image to a single pixel



Sample minutia graph



Identify minutiae



ending minutiae



bifurcation minutiae



Minutia graph

Acceptable score ?



Reference minutia graph for individual



No  
Access denied  
cannot sign record

Yes  
Access to application  
sign records

# Fingerprint



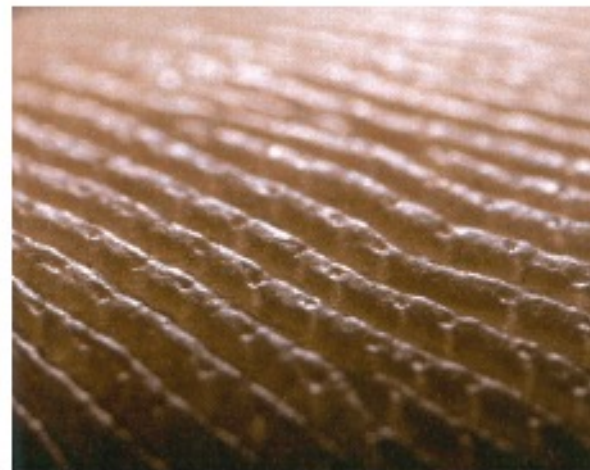
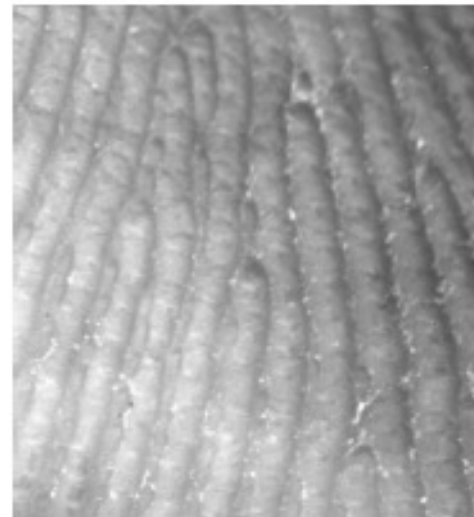
- Fingerprints are "permanent" in that they are formed in the fetal stage, prior to birth, and remain the same throughout lifetime
- The changes can be made by: flexibility from the skin, growing, a dirty finger, scarring, a wound, or a disease of the skin
- They are only weakly determined by genetics, e.g. identical (monozygotic, one egg) twins (the same DNA) have fingerprints that are quite different
- Fingerprints of an individual are "unique"; they indeed are distinctive to a person
- The right definition of a fingerprint is strictly speaking the **print (stamp)** that a finger left on an object



# Fingerprint



- The inside surfaces of hands and feet of humans (and, in fact, all primates) contain minute ridges of skin with furrows between each ridge
- The purpose of this skin structure is to:
  - Facilitate exudation of perspiration
  - Enhance sense of touch
  - Providing a gripping surface



# No fingerprint?



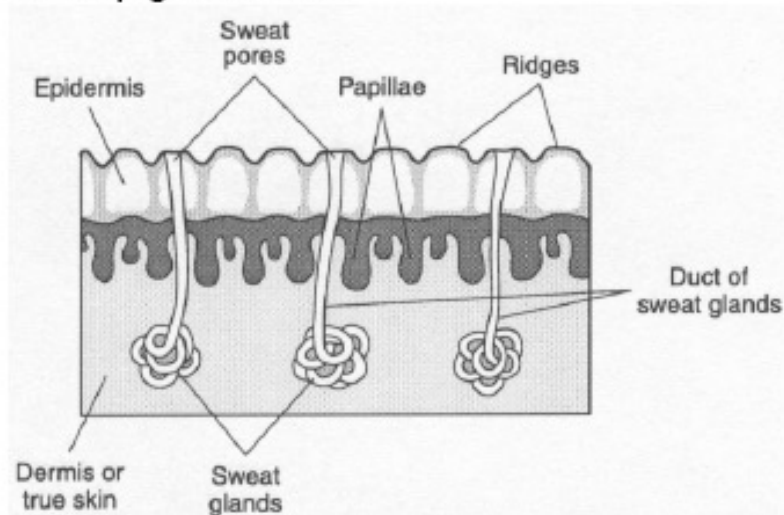
- In very rare cases there are people that do not have prints. Not on their fingers, their palms or their feet. They were born with it or the friction ridges have degenerated during their lives
- Approximately 4% of fingerprint images have been observed to have poor ridge details



# Friction Skin



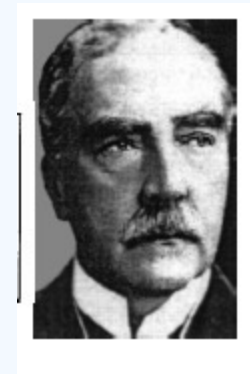
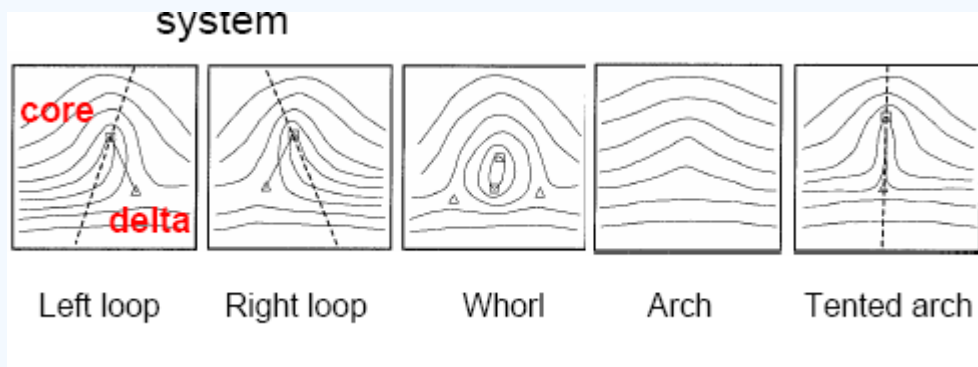
- **Friction skin** differs significantly in structure and function from the skin covering the rest of the body:
  - It is hairless
  - It contains no sebaceous (oil) glands
  - It has a much higher concentration of nerve endings
  - It has a much higher concentration of sweat glands
  - There is a lack of pigmentation



# Fingerprint feature extraction



- Fingerprint pattern, when analyzed at different scales, exhibits different types of features
  - global level - delineates a ridge line flow pattern
    - » Sir Edward Henry 1897
  - local level – minute details can be identified
  - Very fine level – intra-ridge details can be detected





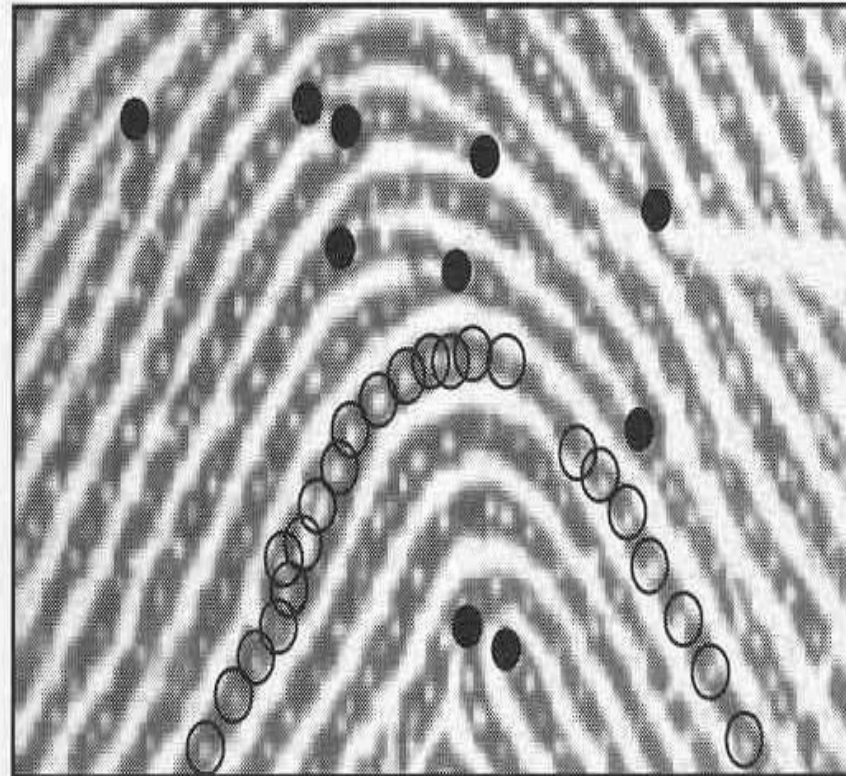


Figure 1.13. Minutiae (black-filled circles) in a portion of fingerprint image; sweat pores (empty circles) on a single ridge line.

# Difficulty in fingerprint matching



- Fingerprint matching is a difficult problem due to large variability in different impressions of the same finger
- Main factors responsible for intra-class variations are: displacement, rotation, partial overlap, non-linear distortion, variable pressure, skin condition, noise and feature extraction errors



Two impressions  
from the same finger



Two impressions  
from different fingers



# Fingerprint classification and Indexing



- To reduce the search time and computational complexity
- technique used to assign a fingerprint to one of the several pre-specified types
- Only a limited number of categories have been identified, and there are many ambiguous fingerprints

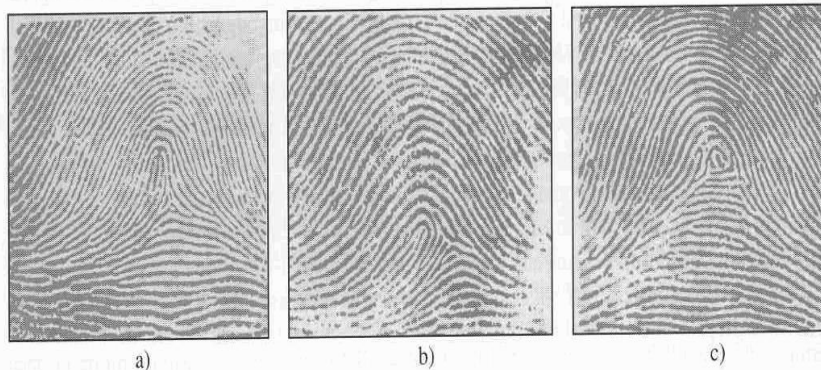


Figure 1.15. Examples of fingerprints that are difficult to classify; a) tented arch; b) a loop; c) a whorl; it seems that all the fingerprints shown here should be in the loop category.



# Latent fingerprint images



10 % visible

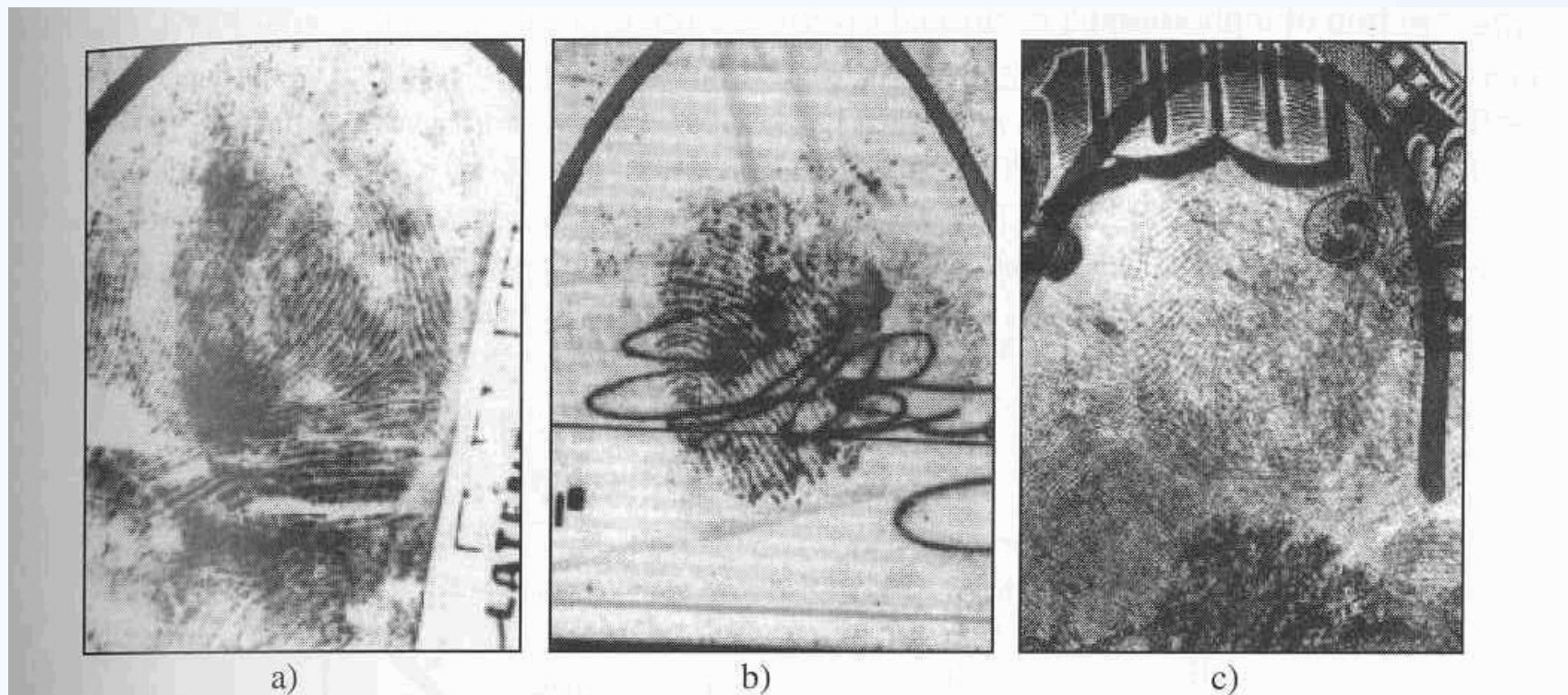


Figure 2.5. Examples of a) good, b) bad, and c) ugly latent fingerprints from NIST Special Database 27 (Garris and McCabe, 2000).



# Enhancement, and Minutias Detection I

**Daniel Novák**

**12.10.2023, Prague**

**Acknowledgments: Xavier Palathingal, Andrzej Drygajlo,  
Handbook of Fingerprint Recognition**



laboratory  
**Gerstner**



## Fingerprint

Interleaved ridges  
and valleys

Ridge width:  $100\mu\text{m}$   
 $300\mu\text{m}$

Ridge-valley cycle:  
 $500\mu\text{m}$

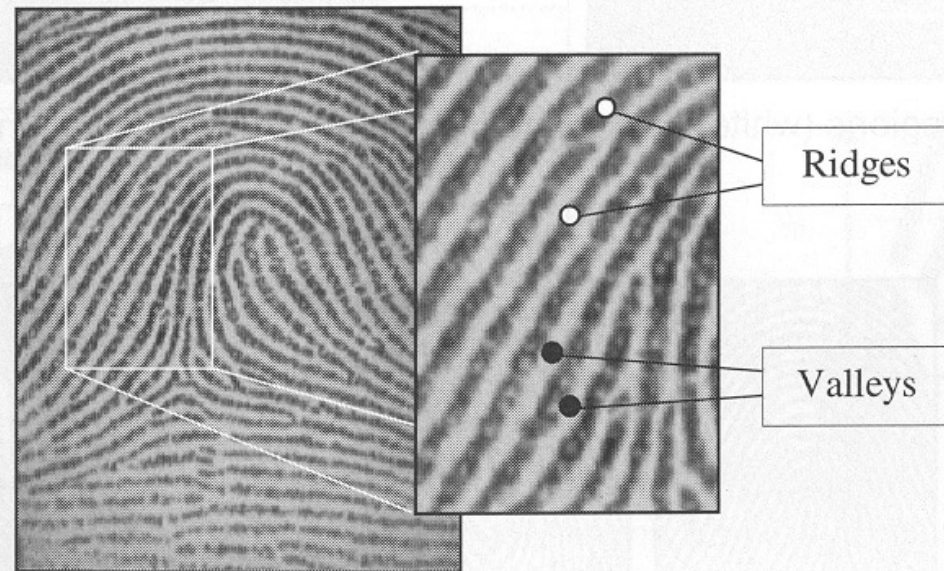


Figure 3.1. Ridges and valleys on a fingerprint image.



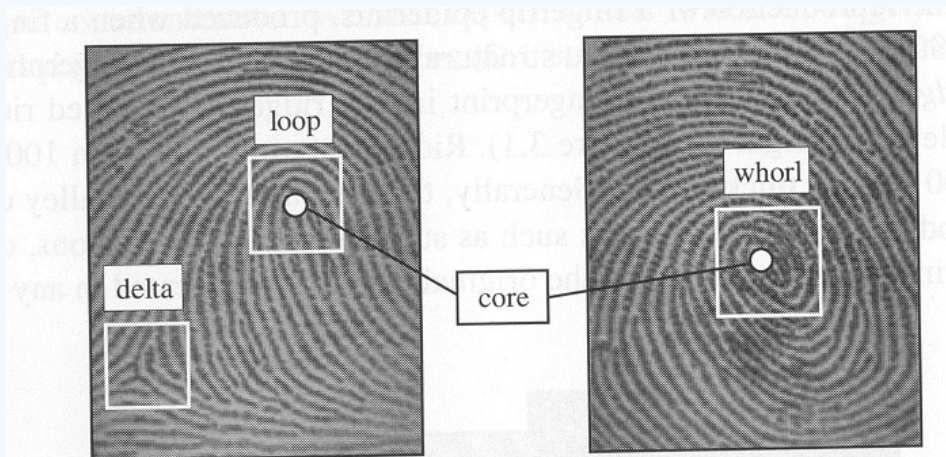
## A Global Look

**Singularities:** In the global level the fingerprint pattern shows some distinct shapes

- Loop ( )
- Delta ( $\Delta$ )
- Whorl (O)...Two facing loop

### **Core:**

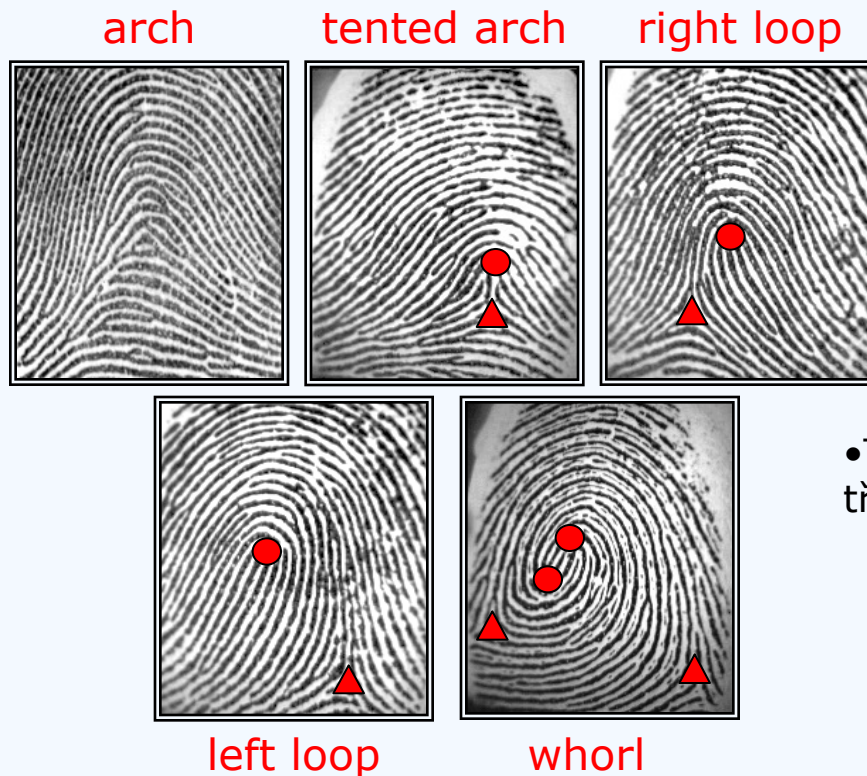
- A reference point for the alignment.
- The northmost loop type singularity.
- According to Henry(1900), it is the northmost point of the innermost ridgeline.
- Not all fingerprints have a core (Arch type fingerprints)





## A Global Look

Singular regions are commonly used for fingerprint classification:



• Tzv Henryho systém, rozděluje otisky do pěti tříd

- Závit (whorl)
- Levá a pravá smyčka (loop)
- Oblouk (arch)
- Špičatý oblouk (tented arch)

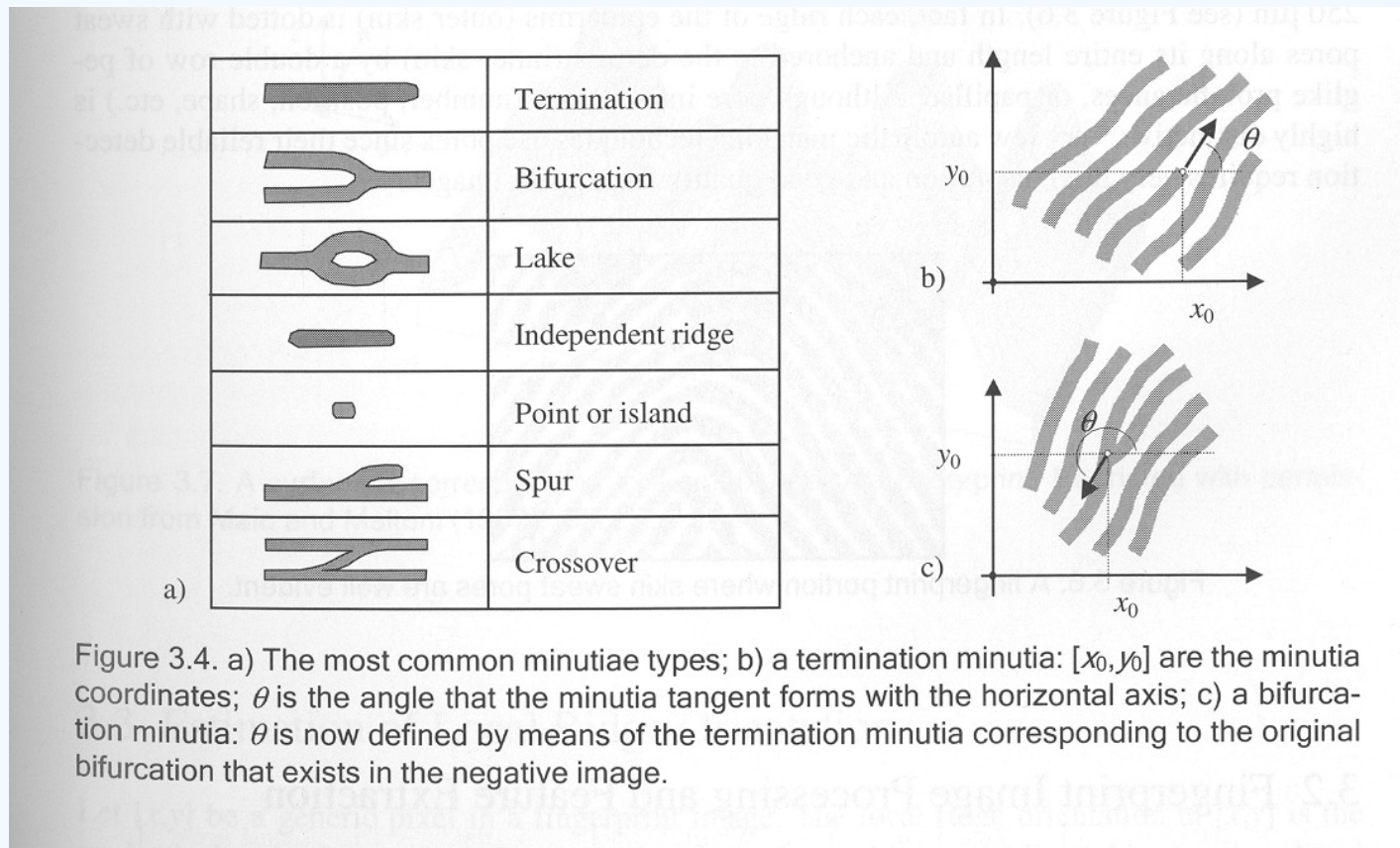






## Local Look

Minutia: Small details. Discontinuities in the ridges. (Sir Francis Galton)



# Terminologie



- Papilární linie
- Vyvýšeniny (ridge)+ prohlubeniny (furrow)
- Charakteristické body
  - Kritické (singulární) body – globálně význačné body
    - Jádro
    - Delt
  - Markanty (Minutiae) – lokálně význačné body
    - Rozvětvení (bifurcation)
    - Zakončení (ridge ending)
    - Krátké hrany (short ridge)
    - Překřížení (crossover, bridge)
    - Krátké rozvětvení (spur)
    - Očka (ridge enclosures)





## Local Look

Ridge ending / ridge bifurcation **duality**

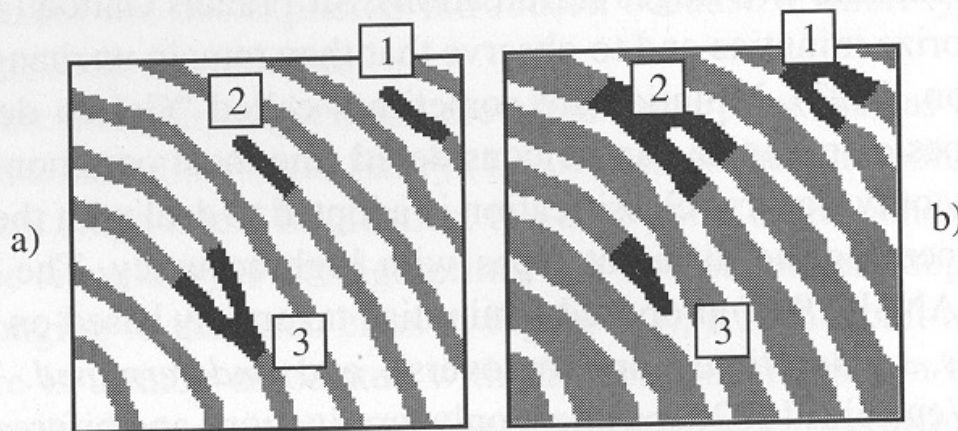


Figure 3.5. The termination/bifurcation duality on a) a binary image and b) its negative image.



# Local Look

## Sweat Pores

- High resolution images (1000 dpi)
- Size 60-250  $\mu\text{m}$
- Highly distinctive
- Not practical (High resolution, good quality images)



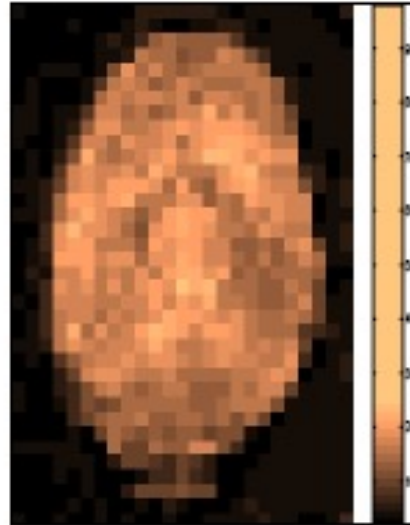
Figure 3.6. A fingerprint portion where skin sweat pores are well evident.



# Segmentation



Original



Variance image



Segmented image

**Segmentation** is the process of isolating foreground from background:

- Image block (16x16 pixels) decomposition
- Thresholding using variance of gradient for each block

# Segmentation



- Separating FP from background
- Straited patterns: no thresholding, striped and oriented pattern & isotropic pattern without orientation
- **Segmentation Methods (16x16 block)**
  - Variance orthogonal to the ridge direction [Ratha95]
    - Assumption: fingerprint area will exhibit high variance, where as the background and noisy regions will exhibit low variance.
    - Variance can also be used as the quality parameter of the regions.
      - High variance (high contrast): good quality
      - Low variance (low contrast): poor quality
  - Average magnitude of gradient in blocks
    - **Fp1 = segmentimage(Fp1);**





# Enhancement, and Minutias Detection II

**Daniel Novák**

**29.9, 2022, Prague**

**Acknowledgments: Xavier Palathingal, Andrzej Drygajlo,  
Handbook of Fingerprint Recognition**



laboratory  
**Gerstner**

# Estimation of Local Ridge Orientation



- Average orientation around indices  $i, j$
- Unoriented directions
- Weighted ( $r_{ij}$ )
- Gradient, maximum pixel-intensity change,  $\arctan gy/gx$

$$\nabla f = \left( \frac{\partial f}{\partial x_1}, \dots, \frac{\partial f}{\partial x_n} \right).$$

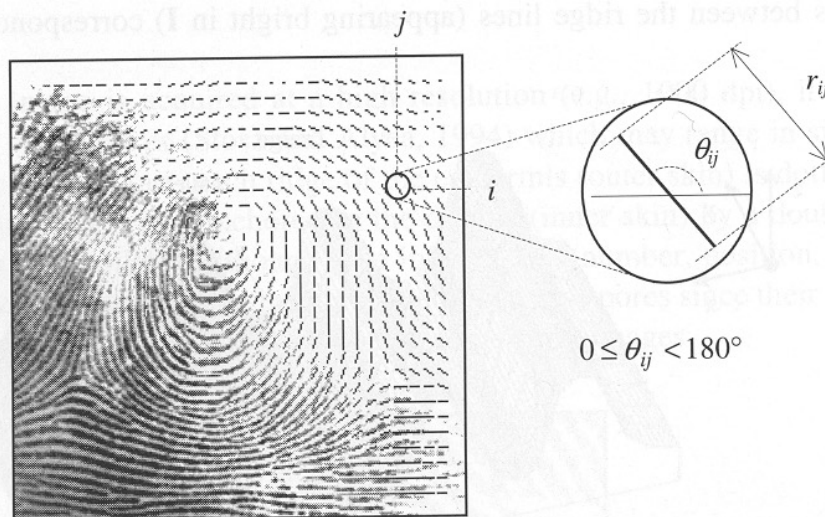


Figure 3.8. A fingerprint image faded into the corresponding orientation image computed over a square-meshed grid of size  $16 \times 16$ . Each element denotes the local orientation of the fingerprint ridges; the element length is proportional to its reliability.





# Estimation of Local Ridge Orientation



## – Simple Approach

- Gradient with Sobel or Prewitt operators
- $\Theta_{ij}$  is orthogonal to the direction of the gradient

$$M_x = \begin{bmatrix} -1 & 0 & 1 \\ -1 & 0 & 1 \\ -1 & 0 & 1 \end{bmatrix} \quad M_y = \begin{bmatrix} -1 & -1 & -1 \\ 0 & 0 & 0 \\ 1 & 1 & 1 \end{bmatrix}$$

$$M_x = \begin{bmatrix} -1 & 0 & 1 \\ -2 & 0 & 2 \\ -1 & 0 & 1 \end{bmatrix} \quad M_y = \begin{bmatrix} -1 & -2 & -1 \\ 0 & 0 & 0 \\ 1 & 2 & 1 \end{bmatrix}$$

## Drawbacks:

Non-linear and discontinuous around 90

A single estimate is sensitive to noise

Circularity of angles: Averaging is not possible

Averaging is not well defined.



# Estimation of Local Ridge Orientation



–Averaging Gradient Estimates

(Kass, Witkin 1987)

$$d_{ij} = [r_{ij} \cdot \cos 2\theta_{ij}, r_{ij} \sin 2\theta_{ij}]$$

$$\bar{\mathbf{d}} = \left[ \frac{1}{n^2} \sum_{i,j} r_{ij} \cdot \cos 2\theta_{ij}, \frac{1}{n^2} \sum_{i,j} r_{ij} \cdot \sin 2\theta_{ij} \right]$$

(2)

$$r = \nabla_x^2 + \nabla_y^2$$



# Estimation of Local Ridge Orientation

## – Effect of averaging

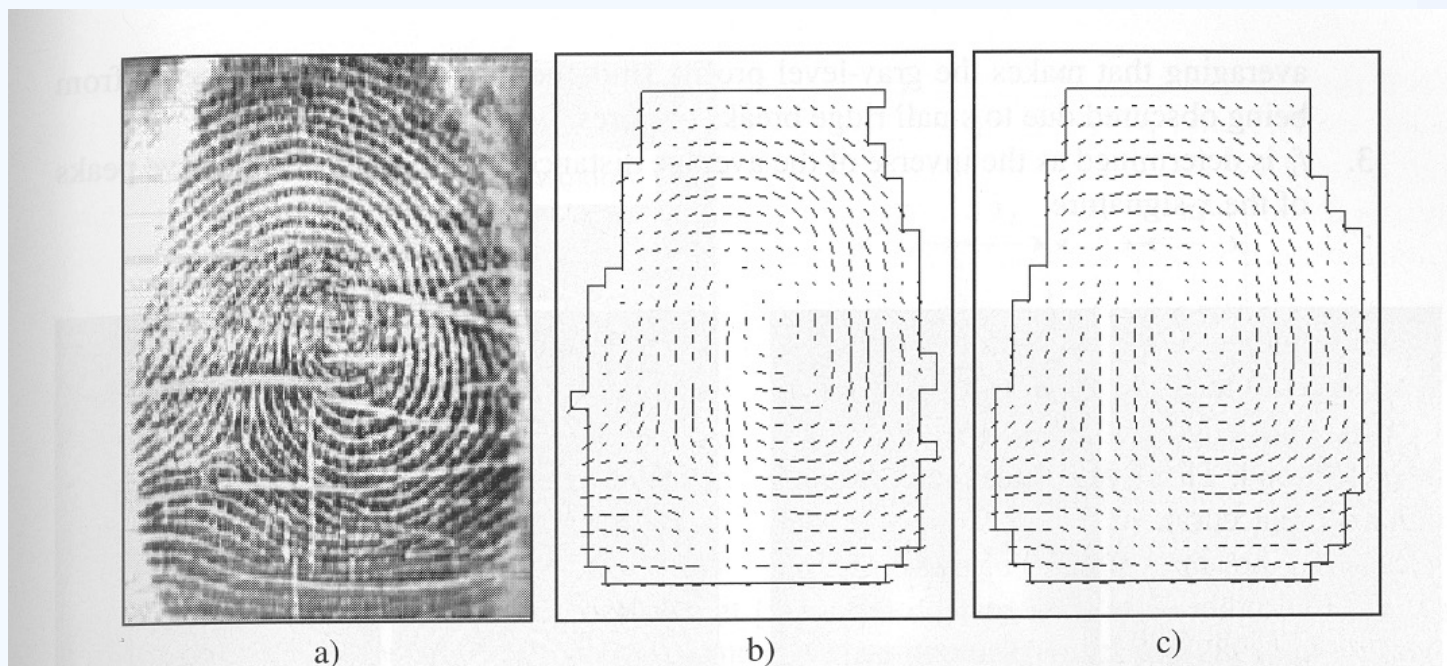


Figure 3.9. a) A poor quality fingerprint image; b) the orientation image of the fingerprint in a) is computed through the Donahue and Rokhlin (1993) method; the orientation of several elements is clearly inconsistent and a regularization step appears necessary; c) the orientation image is the result of the local averaging of each element in b) in its  $3 \times 3$  window according to Equation (2).



# Orientation field



An orientation is calculated for each 16x16 block

- Compute the gradient of the smoothed block.  $G_x(i,j)$  and  $G_y(i,j)$  using 3x3 Sobel Masks
- Obtain the dominant direction in the block using the following equation:

$$\theta_d = \frac{1}{2} \tan^{-1} \left( \frac{\sum_{i=1}^{16} \sum_{j=1}^{16} 2G_x(i,j)G_y(i,j)}{\sum_{i=1}^{16} \sum_{j=1}^{16} (G_x(i,j)^2 - G_y(i,j)^2)} \right), G_x \neq 0 \text{ and } G_y \neq 0 \quad (1)$$

$$G_{xy} = \sum_{h=-8}^8 \sum_{k=-8}^8 \nabla_x(x_i+h, y_j+k) \cdot \nabla_y(x_i+h, y_j+k),$$

$$G_{xx} = \sum_{h=-8}^8 \sum_{k=-8}^8 \nabla_x(x_i+h, y_j+k)^2,$$

$$G_{yy} = \sum_{h=-8}^8 \sum_{k=-8}^8 \nabla_y(x_i+h, y_j+k)^2,$$

$$\theta_{ij} = 90^\circ + \frac{1}{2} \operatorname{atan} 2(2G_{xy}, G_{xx} - G_{yy})$$



- **DEMO: Fp1 = computeorientationarray(Fp1);**
- Gradient is computed by (standard):  $[fx, fy] = \text{gradient}(\text{double}(\text{im}));$
- Block 10x10

# Example: Orientation field

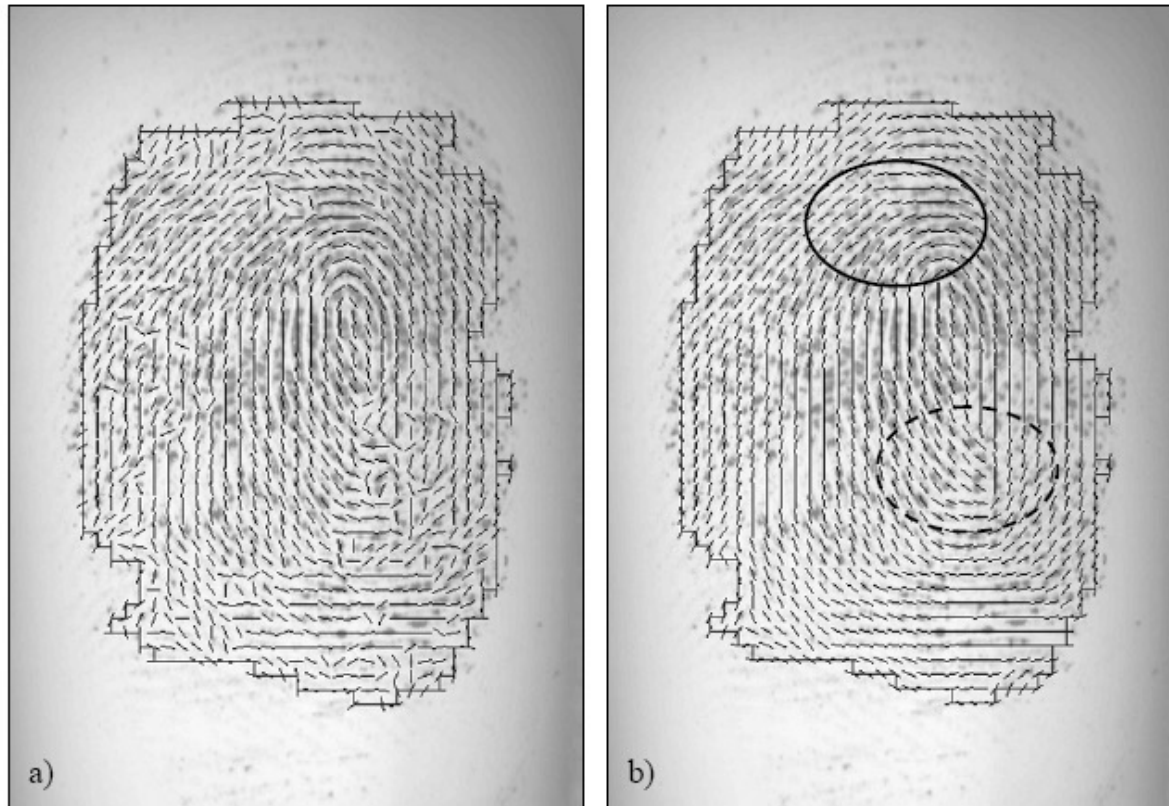
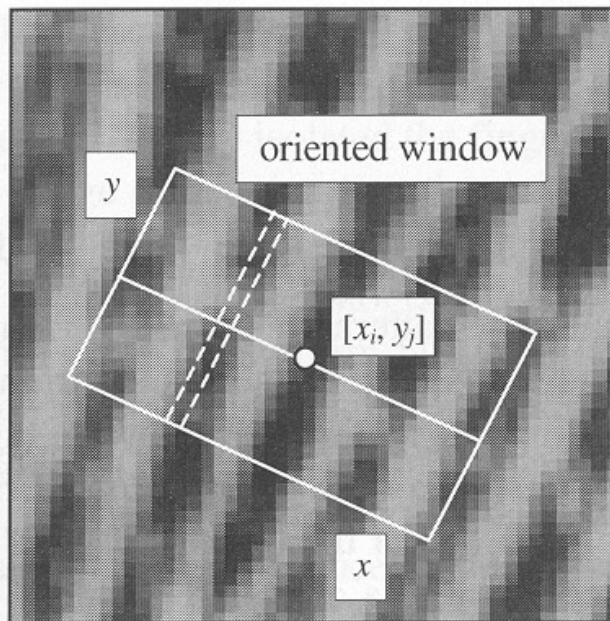


Figure 3.12. a) Estimation of local ridge orientation in a fingerprint through the gradient-based approach corresponding to Equation (3): in the noisy regions the estimation is unreliable; b) two iterations of local (3x3) smoothing are applied, resulting in a more consistent representation; it is worth noting that while the smoothing recovered the correct orientation at several places (e.g., inside the solid circle), it altered the average orientation inside the region denoted by the dashed circle where incorrect orientations were dominating the correct one.



# Estimation of Local Ridge Frequency



$$f_{ij} = \frac{4}{s_1 + s_2 + s_3 + s_4}$$

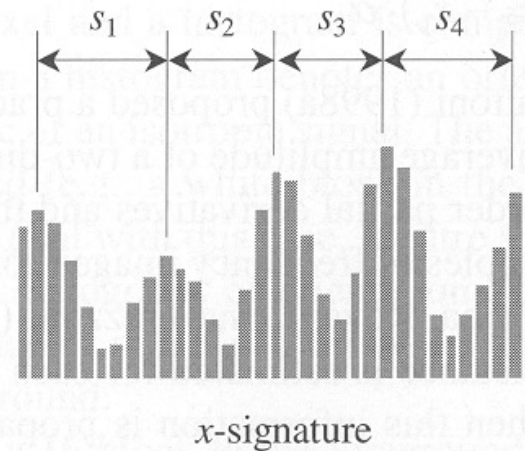


Figure 3.11. An oriented window centered at  $[x_i, y_j]$ ; the dashed lines show the pixels whose gray-levels are accumulated for a given column of the  $x$ -signature (Hong, Wan, and Jain, 1998). The  $x$ -signature on the right clearly exhibits five peaks; the four distances between consecutive peaks are averaged to determine the local ridge frequency.

# Estimation of Local Ridge Frequency



## Simple Algorithm

- 1) 32x16 oriented window centered at  $[x_i, y_i]$
- 2) The x-signature of the grey levels is obtained
- 3)  $f_{ij}$  is the inverse of the average distance

To handle noise interpolation and/or low pass filtering is applied.



**DEMO:** `Fp1 = computelocalfrequency(Fp1, Fp1.imOriginal);`

# Estimation of Local Ridge Frequency



– Examples of frequency maps

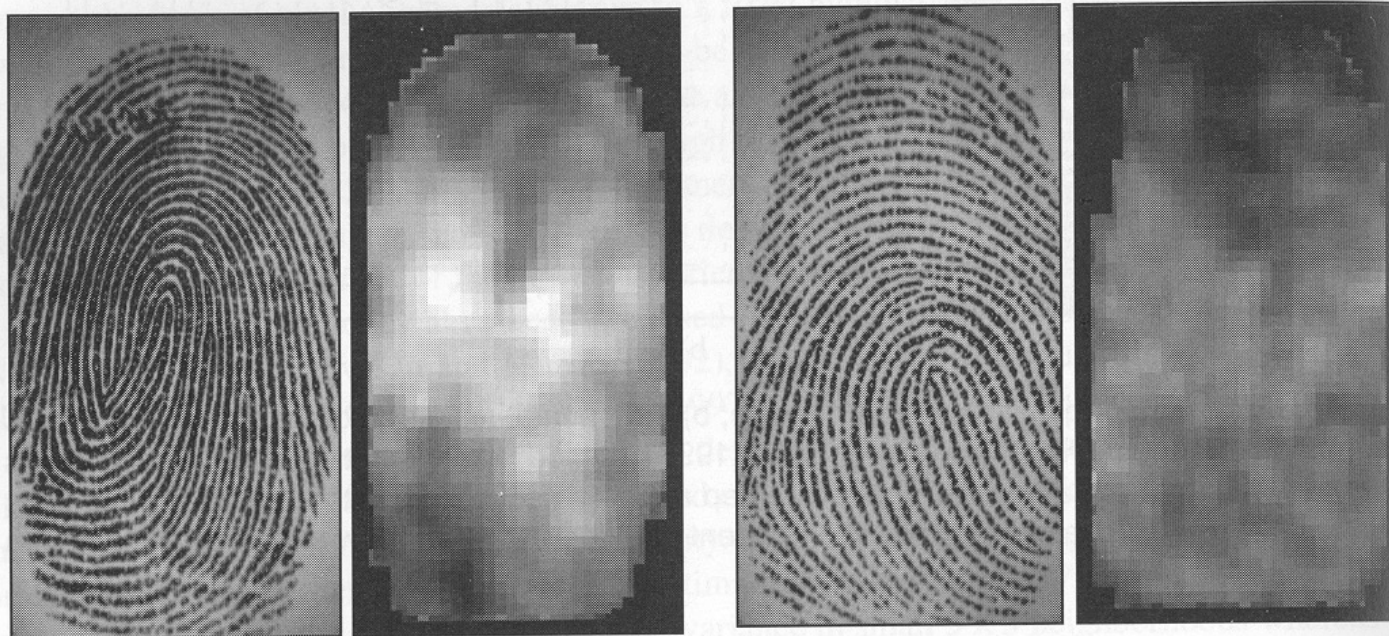


Figure 3.10. Two fingerprint images and the corresponding frequency image computed with the method proposed by Maio and Maltoni (1998a). A local  $3 \times 3$  averaging is performed after frequency estimation to reduce noise. Light blocks denote higher frequencies. It is quite evident that significant changes may characterize different fingerprint regions and different average frequencies may result from different fingers.





# Contextual Filters



- The most widely used technique for fingerprint image enhancement
- Conventional image filtering – a single filter is used for convolution throughout
- Contextual filtering - filter characteristics change according to local context
- Several types of contextual filters proposed
- Indented behavior –
  - 1) provide a low-pass [averaging] effect along the ridge direction.  
*Linking small gaps and filling impurities due to noise*
  - 2) perform a band pass [differentiating] in the direction orthogonal to the ridges  
*Increase discrimination between ridges and valleys*



# Method proposed by Hong, Wan, and Jain



- Based on Gabor filters
- Gabor filters have both frequency-selective and orientation-selective properties and have optimal joint resolution in spatial and frequency domains
- A Gabor filter is defined by a sinusoidal plane wave tapered by a Gaussian

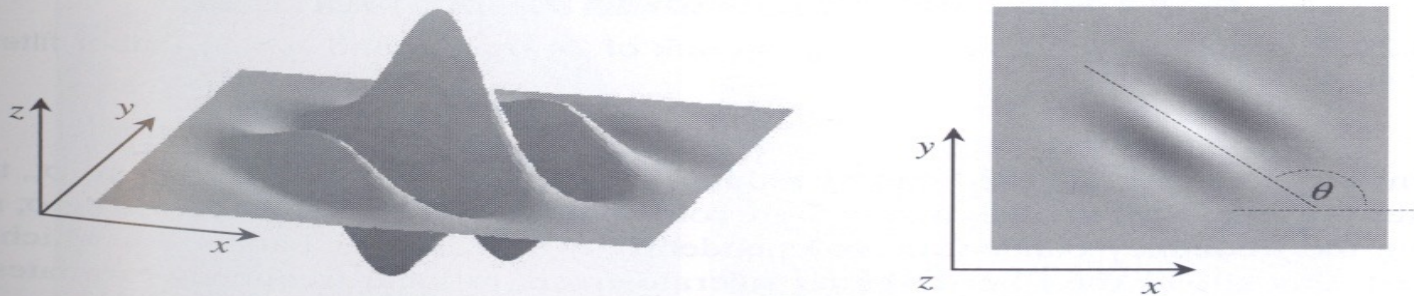


Figure 3.28. Graphical representation (lateral view and top view) of the Gabor filter defined by the parameters  $\theta = 135^\circ$ ,  $f = 1/5$ , and  $\sigma_x = \sigma_y = 3$ .

## Method proposed by Hong, Wan, and Jain (cont ..)



The even symmetric two-dimensional Gabor filter has the following form:

$$g(x, y; \theta, f) = \exp\left\{-\frac{1}{2}\left[\frac{x_\theta^2}{\sigma_x^2} + \frac{y_\theta^2}{\sigma_y^2}\right]\right\} \cdot \cos(2\pi f \cdot x_\theta), \quad (5)$$

where  $\theta$  is the orientation of the filter, and  $[x_\theta, y_\theta]$  are the coordinates of  $[x, y]$  after a clockwise rotation of the Cartesian axes by an angle of  $(90^\circ - \theta)$ .

$$\begin{bmatrix} x_\theta \\ y_\theta \end{bmatrix} = \begin{bmatrix} \cos(90^\circ - \theta) & \sin(90^\circ - \theta) \\ -\sin(90^\circ - \theta) & \cos(90^\circ - \theta) \end{bmatrix} \begin{bmatrix} x \\ y \end{bmatrix} = \begin{bmatrix} \sin\theta & \cos\theta \\ -\cos\theta & \sin\theta \end{bmatrix} \begin{bmatrix} x \\ y \end{bmatrix}.$$

Here,  $f$  is the frequency of a sinusoidal plane wave and  $\sigma_x$  and  $\sigma_y$  are the standard deviations of the Gaussian envelope along the  $x$  and  $y$  axes



# Method proposed by Hong, Wan, and Jain (cont ..)

## Gabor Filter



- 4 parameters –  $\theta, f, \sigma_x, \sigma_y$
- The selection of the values  $\sigma_x$  and  $\sigma_y$  involves a tradeoff
- A set  $\{g_{ij}(x,y) \mid i=1\dots n_0, 1\dots n_f\}$  of filters are priori created and stored, where  $n_0$  is the number of discrete orientations  $\{\theta_i \mid i=1, \dots, n_0\}$  and  $n_f$  the number of discrete frequencies  $\{f_j \mid j=1, \dots, n_f\}$
- Each pixel  $[x,y]$  is convolved, with filter  $g_{ij}(x,y)$  such that  $\theta_i$  is the discretized orientation closest to  $\theta_{xy}$  and  $f_j$  is the discretized orientation closest to  $f_{xy}$
- **DEMO: Fp1 = enhance2ridgevalley(Fp1);**

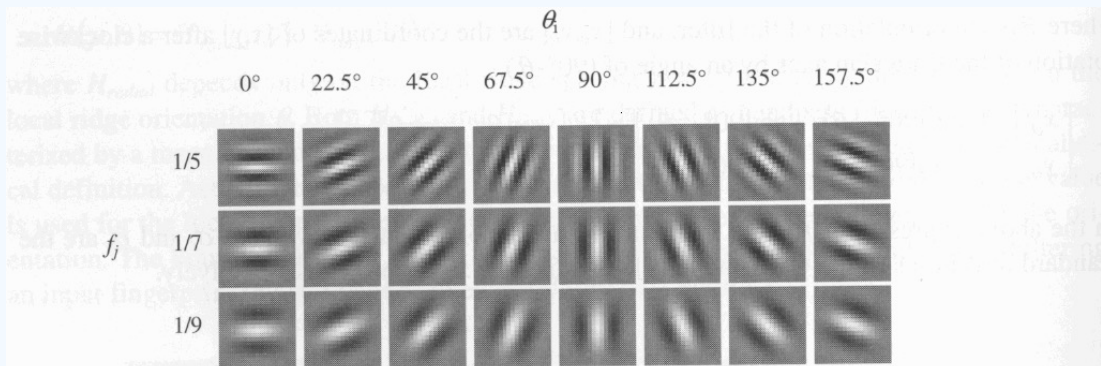


Figure 3.29. A graphical representation of a bank of 24 ( $n_0 = 8$  and  $n_f = 3$ ) Gabor filters where  $\sigma_x = \sigma_y = 4$ .



# Method proposed by Hong, Wan, and Jain (cont ..)

## – Examples



- Shows the application of Gabor-based contextual filtering on medium and poor quality images

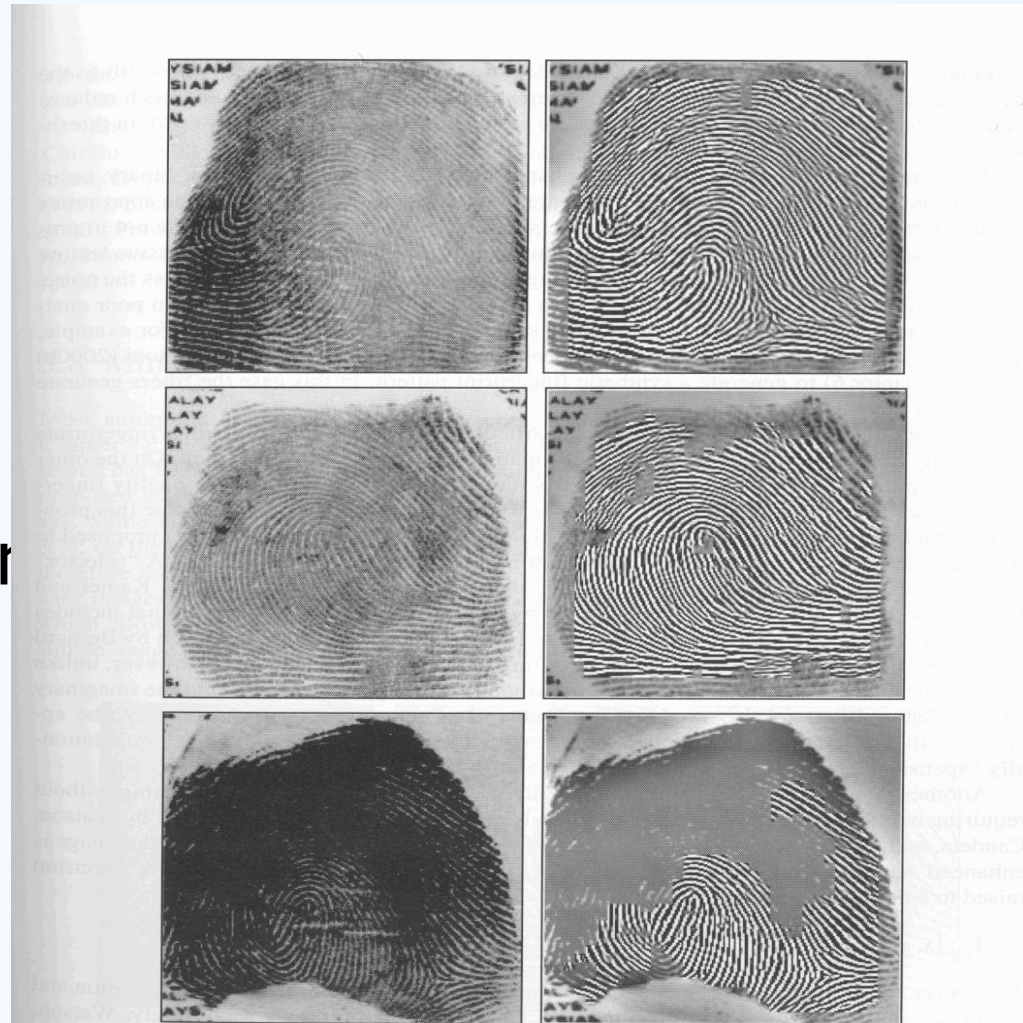


Figure 3.30. Examples of fingerprint enhancement with Gabor filtering as proposed by Hong, Wan, and Jain (1998). On the right, the enhanced recoverable regions are superimposed on the corresponding input images. ©IEEE.



# Minutiae Detection



- Reliable minutiae extraction is extremely important
  - Binarization
  - Thinning
  - Post processing – filling holes, linking breaks, removing bridges

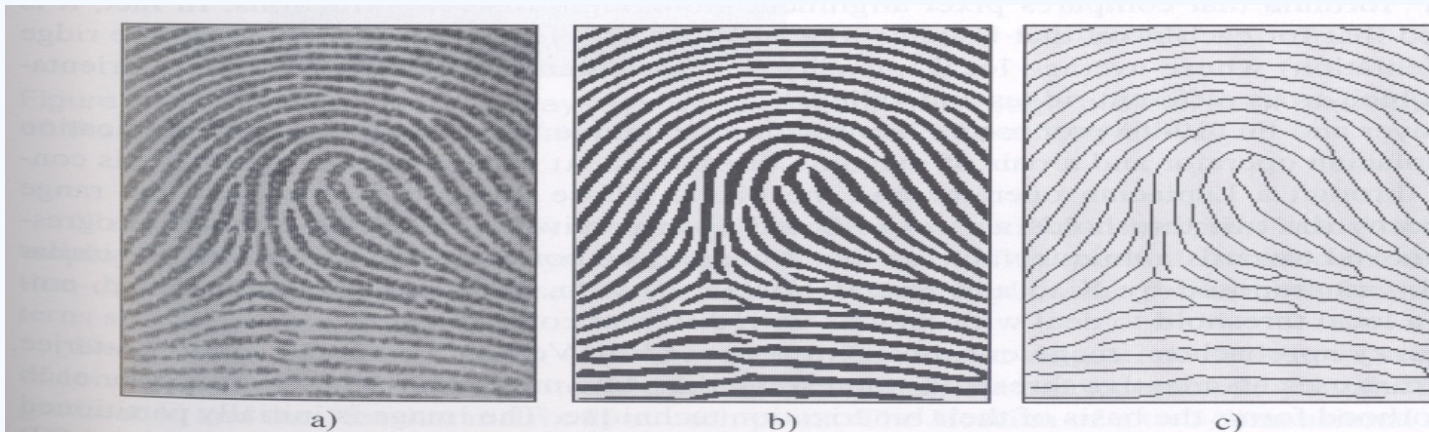


Figure 3.31. a) A fingerprint gray-scale image; b) the image obtained after a binarization of the image in a); c) the image obtained after a thinning of the image in b). Reprinted with permission from Maio and Maltoni (1997). ©IEEE.



# Binarization-based methods



- Simplest method - global threshold
- Local threshold technique
- Fingerprint specific solutions necessary

**Binarization is the output of Contextual Filtering:  
enhance2ridgevalley.m**

```
binaryBlkSize = 20;
```

```
imReconstruct = blkproc(imReconstruct, [binaryBlkSize  
    binaryBlkSize], @binarizeimage);
```

```
function Iout = binarizeimage(Iin)
```

```
level = graythresh(Iin); %Otsu method
```

```
Iout = im2bw(Iin, level);
```





# Threshold computation: Otsu I

- Otsu's method: *N. Otsu (1979). "A threshold selection method from gray-level histograms". IEEE Trans. Sys., Man., Cyber. 9: 62–66*
  - [http://en.wikipedia.org/wiki/Otsu%27s\\_method](http://en.wikipedia.org/wiki/Otsu%27s_method)
  - [http://homepages.inf.ed.ac.uk/rbf/CVonline/LOCAL\\_COPIES/MORSE/threshold.pdf](http://homepages.inf.ed.ac.uk/rbf/CVonline/LOCAL_COPIES/MORSE/threshold.pdf)
- minimizes the intra-class variance – for each threshold  $T$  lot's of work

$$\sigma_{\text{Within}}^2(T) = n_B(T)\sigma_B^2(T) + n_O(T)\sigma_O^2(T)$$

- between-class variance:

$$\begin{aligned}\sigma_{\text{Between}}^2(T) &= \sigma^2 - \sigma_{\text{Within}}^2(T) \\ &= n_B(T) [\mu_B(T) - \mu]^2 + n_O(T) [\mu_O(T) - \mu]^2\end{aligned}$$

$$n_B(T) = \sum_{i=0}^{T-1} p(i)$$

$$n_O(T) = \sum_{i=T}^{N-1} p(i)$$

$\sigma_B^2(T)$  = the variance of the pixels in the background (below threshold)

$\sigma_O^2(T)$  = the variance of the pixels in the foreground (above threshold)

where  $\sigma^2$  is the combined variance and  $\mu$  is the combined mean



# Threshold computation: Otsu II



- Compute histogram and probabilities of each intensity level
- Set up initial  $n_b(0)$  and  $n_o(0)$  and  $\mu_b(0)$ ,  $\mu_o(0)$
- Step through all possible thresholds  $T=1 \dots$  maximum intensity
  - Update  $n_b(T), n_o(T)$
  - Compute  $\sigma_{\text{between}}(T)$
- Desired threshold corresponds to the maximum  $\sigma_{\text{between}}(T)$



# Minutiae detection

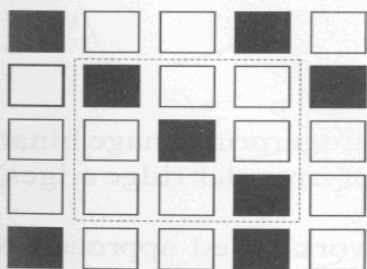


- A simple image scan allows the pixel corresponding to minutiae to be detected
- *crossing number* of a pixel  $p$
- **DEMO: Fp1 = cleanskeleton(Fp1);**

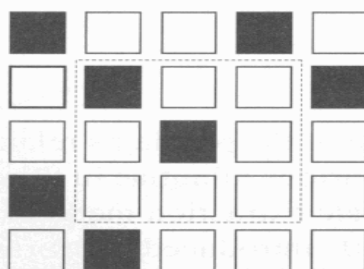
$$cn(\mathbf{p}) = \frac{1}{2} \sum_{i=1..8} |val(\mathbf{p}_{i \bmod 8}) - val(\mathbf{p}_{i-1})|,$$

where  $\mathbf{p}_0, \mathbf{p}_1, \dots, \mathbf{p}_7$  are the pixels belonging to an ordered sequence of pixels defining the 8-neighborhood of  $\mathbf{p}$  and  $val(\mathbf{p}) \in \{0,1\}$  is the pixel value. It is simple to note (Figure 3.36) that a pixel  $\mathbf{p}$  with  $val(\mathbf{p}) = 1$ :

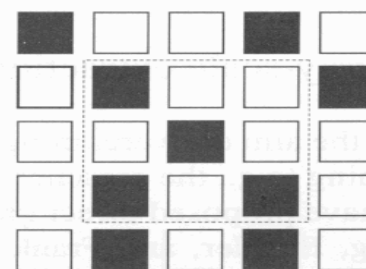
- is an intermediate ridge point if  $cn(\mathbf{p}) = 2$ ;
- corresponds to a termination minutia if  $cn(\mathbf{p}) = 1$ ;
- defines a more complex minutia (bifurcation, crossover, etc.) if  $cn(\mathbf{p}) \geq 3$ .



a)  $cn(\mathbf{p}) = 2$



b)  $cn(\mathbf{p}) = 1$



c)  $cn(\mathbf{p}) = 3$

Figure 3.36. a) intra-ridge pixel; b) termination minutia; c) bifurcation minutia.





# Examples of minutiae extraction

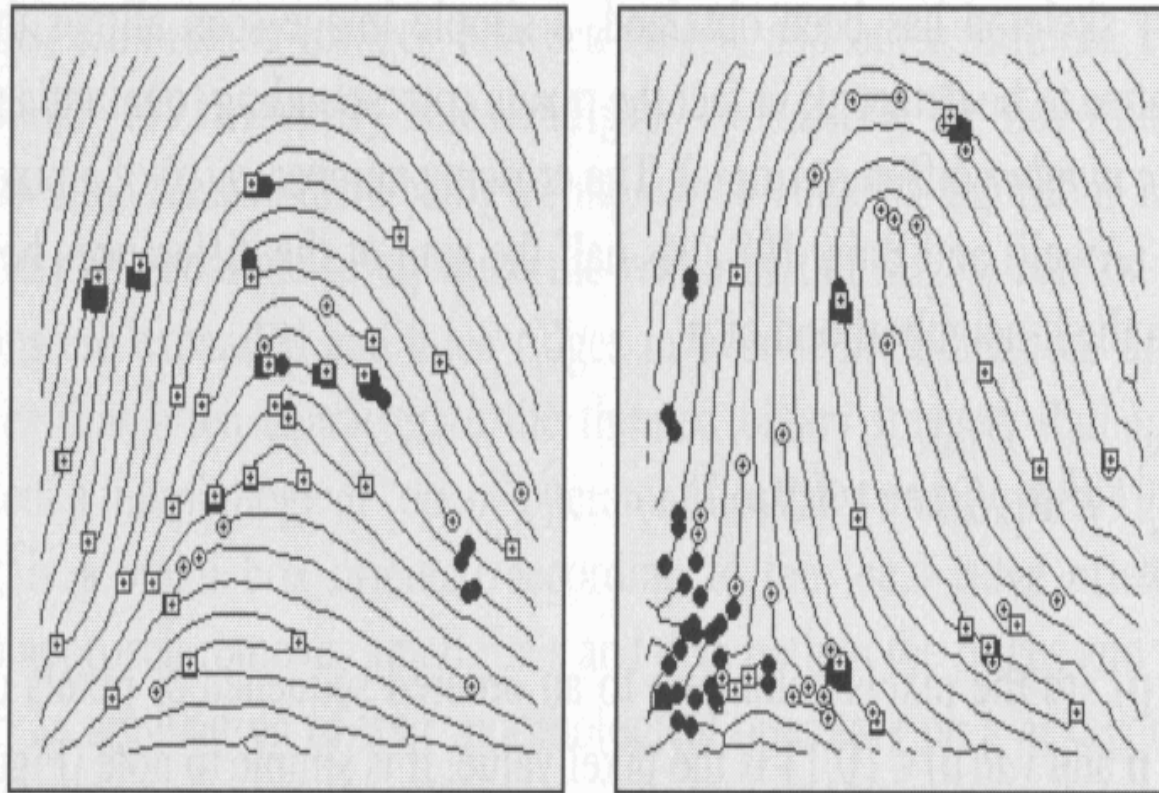
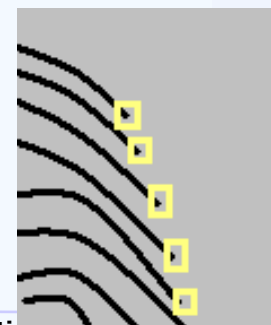
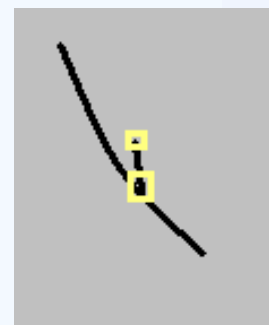
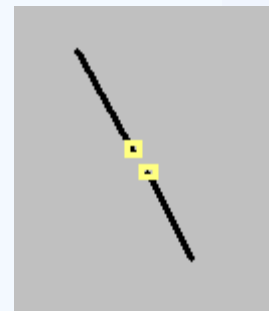


Figure 3.37. Examples of minutiae detection on binary skeletons. White circles and white boxes denote terminations and bifurcations, respectively; black circles and black boxes denote filtered minutiae (see Section 3.9).



# Minutiae Filtering

- Post-processing stage is useful for removing spurious minutiae [already present or introduced by previous steps]
- Two main post-processing types:
  - Structural post-processing
  - Minutiae filtering in the gray-scale domain
- Ridge breaks (insufficient ink or moist)
- Ridge cross-connections (over-ink, over-moist)
- Boundaries



# Example

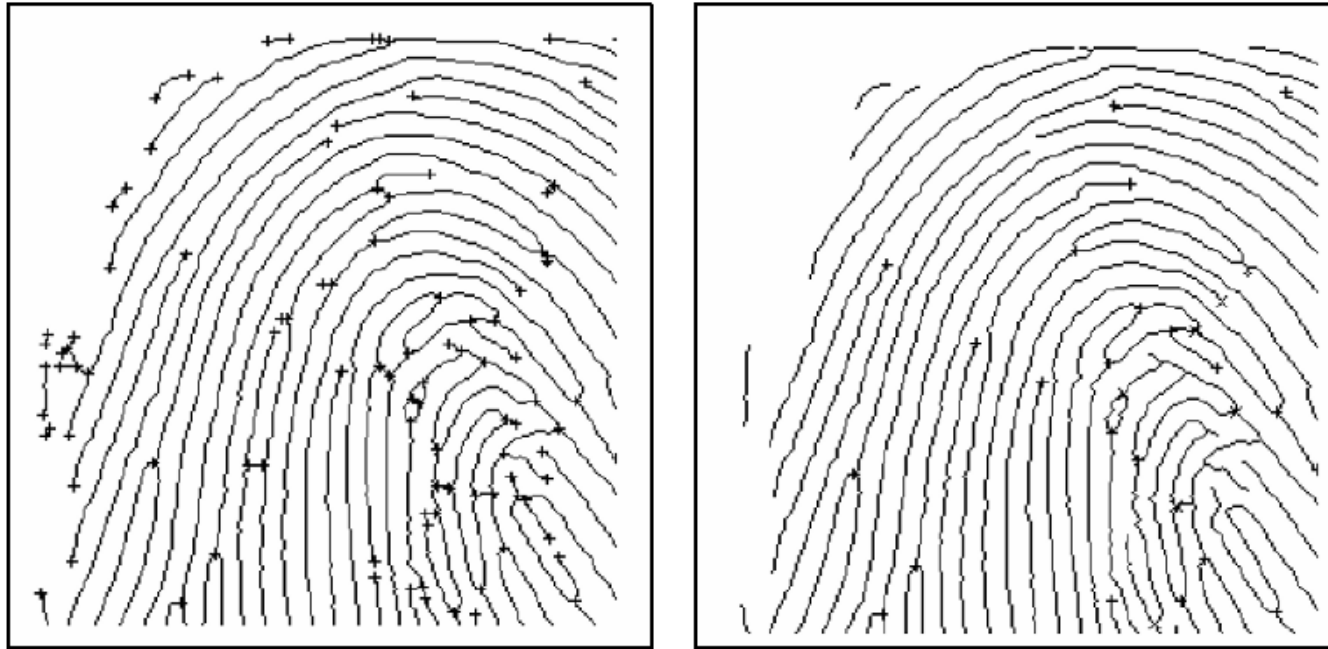


Figure 3.51. Minutiae post-processing according to Farina, Kovacs-Vajna, and Leone (1999). On the right, most of the false minutiae present in the thinned binary image (on the left) have been removed. © Elsevier.